

Taylor & Francis
Taylor & Francis Group

Molecular Physics

An International Journal at the Interface Between Chemistry and Physics

ISSN: 0026-8976 (Print) 1362-3028 (Online) Journal homepage: www.tandfonline.com/journals/tmph20

Structural characterisation of hydrolysed Cm(III)-EDTA solution species under alkaline conditions: a TRLFS, vibronic side-band and quantum chemical study

M. Trumm, A. Tasi, A. Schnurr, N. A. DiBlasi & X. Gaona

To cite this article: M. Trumm, A. Tasi, A. Schnurr, N. A. DiBlasi & X. Gaona (2022) Structural characterisation of hydrolysed Cm(III)-EDTA solution species under alkaline conditions: a TRLFS, vibronic side-band and quantum chemical study, Molecular Physics, 120:8, e2033864, DOI: 10.1080/00268976.2022.2033864

To link to this article: https://doi.org/10.1080/00268976.2022.2033864

Published online: 05 Feb 2022.

Submit your article to this journal

Article views: 165

View related articles

View Crossmark data

Citing articles: 1 View citing articles

Full Terms & Conditions of access and use can be found at
https://www.tandfonline.com/action/journalInformation?journalCode=tmph20

MOLECULAR PHYSICS
2022, VOL. 120, NO. 8, e2033864 (7 pages)
https://doi.org/10.1080/00268976.2022.2033864

Taylor & Francis
Taylor & Francis Group

RESEARCH ARTICLE

Check for updates

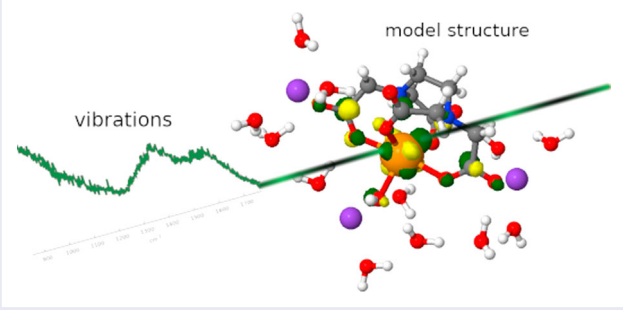
Structural characterisation of hydrolysed Cm(III)-EDTA solution species under alkaline conditions: a TRLFS, vibronic side-band and quantum chemical study

M. Trumm [a], A. Tasi[a], A. Schnurr[a], N. A. DiBlasi[a,b] and X. Gaona[a]

[a]Institut für Nukleare Entsorgung (INE), Karlsruher Institut für Technologie, Karlsruhe, Germany; [b]Department of Civil & Environmental Engineering & Earth Sciences, University of Notre Dame, Notre Dame, IN, USA

ABSTRACT

We present a combined theoretical and experimental study of the Cm(III)-EDTA system in alkaline aqueous solutions. Time-resolved laser-fluorescence spectroscopy and vibronic side-band spectroscopy measurements are performed with $[Cm] = 10^{-7}M$, $[EDTA]_{tot} = 10^{-3}M$ and $7 \leq pH \leq 12$. The evaluation of the TRLFS spectra and corresponding fluorescence lifetimes hints towards the predominance of $Cm(EDTA)^{-}$ at $pH = 7$, with the subsequent formation of the hydrolysis species $Cm(OH)_n(EDTA)^{-1-n}$ with increasing pH. This speciation scheme is further supported by the excellent agreement obtained between experimental and calculated vibronic side bands. The relative stabilities of the complexes $Cm(OH)_n(EDTA)_p^{3-n-4p}$ with $n = 0-2$ and $p = 1-2$ are discussed on the basis of the equilibrium constants calculated from quantum chemical calculations.



ARTICLE HISTORY
Received 12 March 2021
Accepted 14 January 2022

KEYWORDS
Vibrational spectroscopy; laser-fluorescence spectroscopy; quantum chemistry; actinide chemistry

1. Introduction

Solubility phenomena and sorption processes of radionuclides can be strongly affected by their interaction with organic ligands. To assess the potential impact of these complexes on the retention and mobilisation of radionuclides in a repository for nuclear waste, profound knowledge of the chemical and thermodynamic models of relevant actinide ions with the specific ligands is necessary. Ethylenediaminetetraacetic acid (H_4EDTA) is adapted to differentiate between various degrees of its protonation state, see Figure 1 for the molecular structure) is known to form stable complexes with tri- and tetravalent actinides. A number of experimental studies available in the literature are dedicated to the complexation of Cm(III) with H_4EDTA [1–9]. Most of these studies report only the formation of the 1:1 complex $Cm(EDTA)^{-}$, although the predominance of the protonated species Cm(HEDTA)(aq) is also proposed below pH ≈ 2.5 [2, 4]. Recent spectroscopic studies also provide evidence on the formation of the ternary complex $Cm(OH)(EDTA)^{2-}$ in alkaline systems with pH above ≈9 [7, 8]. In contrast to the complexes forming in acidic conditions, no thermodynamic data has been reported so far for $Cm(OH)(EDTA)^{2-}$. The formation of the analogous Am(III) complexes Am(HEDTA)(aq) and $Am(EDTA)^{-}$ under acidic conditions has been extensively proven by different experimental methods (cation exchange, solvent extraction, electromigration or spectrophotometry, among others) [1, 2, 6–16]. Based on the changes in the rate of electromigration of Am(III) in the presence of EDTA, Shalinets proposed the formation of the ternary complex $Am(OH)(EDTA)^{2-}$ above

CONTACT M. Trumm Michael.Trumm@kit.edu Institut für Nukleare Entsorgung (INE), Karlsruher Institut für Technologie, Karlsruhe 76131, Germany

© 2022 Informa UK Limited, trading as Taylor & Francis Group

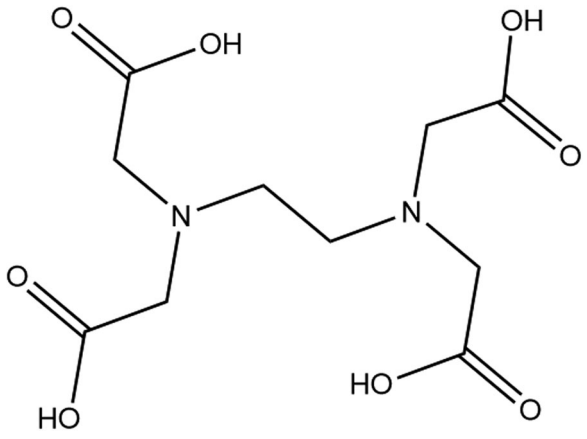


Figure 1. Molecular structure of the H_4EDTA molecule.

pH $\approx$10 [4]. In a series of spectroscopic experiments, Delle Site and co-workers investigated the complexation of Am(III) with EDTA within $1 \leq pH \leq 12$ and $1 \cdot 10^{-3}M \leq [EDTA]_{tot} \leq 5 \cdot 10^{-2}M$ ($[EDTA]_{tot}$ denotes the total concentration of the ligand in molar units accounting for all of its protonated forms) [12]. The authors reported the formation of the complexes $Am(EDTA)^-$, $Am_2(EDTA)_3^{6-}$ and $Am(EDTA)_2^{5-}$ at pH $\approx$ 1.0–2.1, $\approx$ 3.75–7.25 and $\approx$ 7.0–12.0, respectively. Within the boundary conditions of their experiment (with $[EDTA]_{tot} \leq 5 \cdot 10^{-2}M$), Delle Site et al. observed only the weak formation of the 1:2 complex, and indicated also the expected co-existence of a complex involving the partial hydrolysis of the Am(III) ion. We note also that the experiments in [12] were conducted at $[Am(III)] = 1 \cdot 10^{-3}M$, for which the precipitation of $Am(OH)_3$(am) is expected in alkaline systems even at high EDTA concentrations.

Extensive theoretical studies of metal EDTA complexes can be found in literature, but structures involving trivalent actinides or lanthanides are scarce. Heathman et al. report structures of aqueous $Eu(EDTA)^-$ complexes from density functional theory (DFT) and ab initio molecular dynamics (AIMD) [17]. However, the formation of hydroxo complexes has up to this point not been investigated with ab initio methods. This manuscript will provide strong evidence for the formation of $Cm(OH)(EDTA)^{2-}$ and higher hydrolysis species. A thorough investigation by means of time resolved laser-fluorescence spectroscopy (TRLFS), vibronic sideband spectroscopy (VSBS) and quantum chemical calculations is performed, providing detailed structural and thermodynamic data on the Cm/EDTA 1:1 and 1:2 complexes, such as bond distances, stability constants, reaction enthalpy and -entropy in the pH range 7–12.

2. Experimental setup and theoretical model

2.1. Chemicals and sample preparation

All experiments were performed under argon atmosphere with the exclusion of CO_2 and O_2 (< 2 ppm) at KIT-INE laboratories. Solutions were prepared using ultra pure water purified with a Milli-Q apparatus (Millipore, 18.2 MΩ, $22 \pm 2°C$). Prior to its application, Milli-Q water was boiled for several hours while being purged with argon gas. EDTA-containing solutions were prepared by mixing its sodium salts (Sigma Aldrich) accounting for the speciation evolution of the deprotonated species: H_4EDTA (purity $\leq$ 98.5%), Na_2H_2EDTA (99.0-101.0%), Na_3HEDTA·xH_2O ($\leq$ 95%), and Na_4EDTA·$2H_2O$ (99.0-101.0%). A stock solution with an isotopic composition of 89.68 % ^{248}Cm, 9.38 % ^{246}Cm, 0.43 % ^{243}Cm, 0.30 % ^{244}Cm, 0.14 % ^{245}Cm and 0.07 % ^{247}Cm at a total concentration of $[Cm]_{tot} = 10^{-7}$ M in 0.001–0.01 M HCl media was used as curium source. Final adjustment of the pH in the target solution was performed by the addition of 0.1 M NaOH or HCl standard solutions (Merck, Titrisol). Between each titration step, samples were allowed to equilibrate for 24 h before the final pH values and corresponding spectra were collected.

2.2. TRLFS and VSBS setup

Time-resolved laser fluorescence (TRLFS) measurements were performed using a Nd-YAG pumped dye (Exalite 398) laser system (NARROWscan D-R Dye Laser) with a repetition rate of 10 Hz. Cm(III) was excited at a wavelength of 396.6 nm with a pulse energy of 2–4 mJ. Emission spectra were recorded between 575 nm and 635 nm after a delay time of 1 μs (gate width 10 ms). After spectral decomposition by a spectrograph (Shamrock 303i) with 1199 lines per mm grating, the spectra were recorded with an ICCD camera (iStar Gen III, ANDOR) containing an integrated delay controller. Fluorescence lifetime measurements were performed by recording the emission spectra as a function of increasing delay time (with steps of 10–40 μs) between laser pulse and camera detection. The fluorescence emission lifetime (τ) was obtained by fitting the integrated intensity (I) (and also the absolute intensity at peak maxima positions) as a function of delay time (t) following $I(\lambda) = I_0(\lambda)exp(-t/\tau)$, where I_0 is the intensity at $t = 0$. To measure vibronic side bands, Cm(III) emission spectra were recorded by increasing the central wavelength in 10 nm intervals up to about 860 nm using 1199 lines per mm grating. Vibrational energies were calculated using the positions of the vibronic side bands relative to the zero

phonon line (ZPL), which is the main ${}^6D'_{7/2} \rightarrow {}^8S'_{7/2}$ transition of Cm(III):

$$\nu_{vib} = \nu_{ZPL} - \nu_{side\ band} \quad (1)$$

2.3. Structure optimisation and vibrational spectra

Density functional theory employing the B3LYP [18, 19] functional was used to optimise structures of $[Cm(OH)_n(H_mEDTA)_p]^{3-n-p(4-m)}$ complexes with $m = 0$, 1, 2 and 4, $n = 0{-}2$, and $p = 1{-}2$. The B3LYP functional has shown to give reasonable molecular structures for actinide complexes in earlier studies.

Cm was described by a small-core pseudo potential ECP60MWB with corresponding basis sets of triple-zeta quality [20]. All other atoms were described by the def2-TZVP basis sets as implemented in the TURBOMOLE software package [21]. After the structure optimisation, all geometries were proven to be true minima by vibrational frequency calculation. Vibronic side-band spectra are obtained from the computed vibrational frequencies by scaling the vibrational modes by r^{-6}, with r being the atomic distances of the involved atoms to the Cm(III) ion.

2.4. Energy calculations

Gibbs energies for the complexation reactions have been computed according to a thermodynamic cycle:

$$\Delta G = \Delta E_g + \Delta E_{zp} + \Delta H - T\Delta S + \Delta E_{solv} \quad (2)$$

where E_g represents the gas-phase energies, E_{zp} is the zero-point energy, H and S represent enthalpy and entropy as determined from the vibrational frequencies and E_{solv} is the solution energy computed using the conductor-like screening model COSMO [22] with a cavity radius of 1.72 Å for Cm(III). Additionally, corrections for hydrogen bonds [23] and standard state [24] have been applied to ΔG.

Values for ΔG, ΔH, $-T\Delta S$ and log K have been computed for the complexation reactions

$$Cm(OH)^{2+}(aq) + H_2EDTA^{2-}(aq) \rightleftharpoons Cm(H_mEDTA)^{m-1}(aq) + (1-m)^{+}(aq) + H_2O(l) \quad (3)$$

$$Cm(EDTA)^{m-1}(aq) + H_2EDTA^{2-}(aq) \rightleftharpoons Cm(H_mEDTA)_2^{2m-5}(aq) + (2-2m)H^{+}(aq) \quad (4)$$

as well as for the formation of the ternary complexes $[Cm(OH)_n(H_mEDTA)]^{m-n-1}$

$$Cm(OH)^{2+}(aq) + H_2EDTA^{2-}(aq) \rightleftharpoons Cm(OH)(H_mEDTA)^{m-2}(aq) + (2-m)H^{+}(aq) \quad (5)$$

$$Cm(OH)^{2+}(aq) + H_2EDTA^{2-}(aq) + H_2O(l) \rightleftharpoons Cm(OH)_2(H_mEDTA)^{m-3}(aq) + (3-m)H^{+}(aq) \quad (6)$$

3. Results

3.1. Fluorescence measurements

Normalised Cm(III) TRLFS spectra in the presence of $[EDTA]_{tot} = 10^{-3}$ M depict one isosbestic point as a function of pH indicating the equilibrium between two dominant species (see supporting information Figure SI.1) with peak maxima positions of 603.9 and 606.9 nm. In the absence of EDTA, the dominant Cm-species are Cm^{3+} and $Cm(OH)^{2+}$ up to pH $\approx$ 9 [25]. Hence, the peak at 603.9 nm can only be associated with the $Cm(EDTA)^{-}$ binary complex as also reported by Thakur et al. [7]. The fluorescence lifetime of 231±41 μs of the given species was found to be larger in contrast to the 64±41 μs of the aquo ion (λ_{max} = 593.8 nm) as well as the 76±2 and 80±20 μs of $Cm(OH)^{2+}$ (λ_{max} = 598.7 nm) and $Cm(OH)_2^{+}$ (λ_{max} = 603.5 nm), respectively. Following the equation of Kimura [26], this value translates to a decreased average number of N_{H2O} = 2.1±0.7 water molecules in the first coordination shell of the complex. The lifetime of the second species emerging at 606.9 nm with increasing pH was determined to be 332±41 μs yielding N_{H2O} = 1.1±0.3. Upon further increase in pH, although to lesser extent, the formation of a third species can be seen with a peak maximum at 613.9 nm. Experimental observations collectively hint towards the gradual formation of hydrolysed $Cm(OH)_n(EDTA)^{-1-n}$ species, as previously described for other M(III)- and M(IV)-EDTA systems, e.g. Fe(III), Th(IV) or Pu(IV) species [27–29].

3.2. Vibronic side bands

Spectra of the vibronic side bands obtained under pH = 7–12 referenced to positions of the individual ZPLs are shown in Figure 2. In all cases, three spectral features were identified around 950, 1400 and 1600 cm^{-1}. The well-defined red shift of the spectra by 20–30 cm^{-1} observed as a function of pH can be attributed to the change in solution speciation. Whilst the spectra at pH = 7 and 9 are indistinguishable, at pH = 11 and 12, a

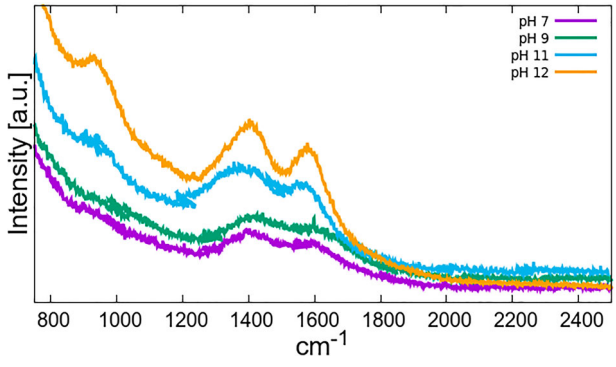


Figure 2. Measured vibronic side-band spectra for the Cm(III)-EDTA system as a function of pH = 7, 9, 11 and 12.

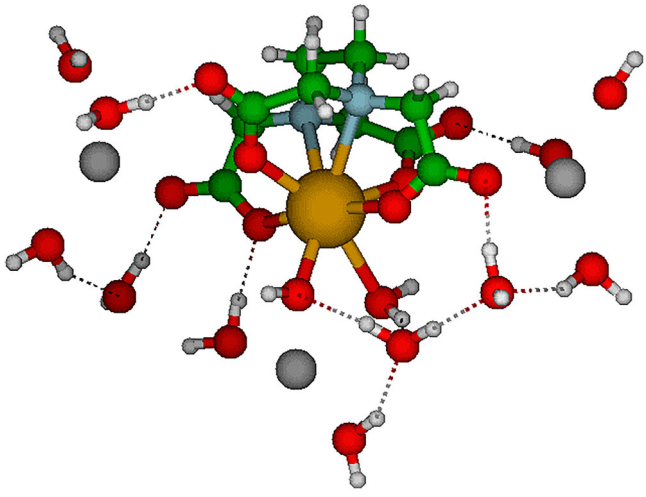


Figure 3. Structure of the $[Cm(OH)(H_2O)(EDTA)]^{2-} \cdot [(Na(H_2O)_4)_3]^{3+}$ complex. Cm (brown), O (red), N (blue), C (green), H (white), Na (grey).

new dominant species is present showing vibrational side bands with seemingly increasing intensity. Based on the small magnitude of the observed shift, the two species are likely to share structural similarities. Note also, that the water bending mode is located around 1650 cm^{-1}, capable of contributing to the intensity of the 1600 cm^{-1} side band (see, i.e. [30]). However, owing to the small amount of water molecules in the first coordination shells of the complexes, water vibrations are expected to play only a minor role in the present system.

3.3. Computed structures and energies

Geometric properties of the optimised structures without Na^+ counterions can be found in the supporting information (Tables SI.1 and SI.2). All relevant structures have been saturated by multiple $[Na(H_2O)_4]^+$ clusters to simulate experimental conditions. Bond distances are listed in Table 3. Cm-N distances are substantially longer and more sensitive to ligand configuration and water interaction. Computed Cm-EDTA bond lengths are about 4 pm shorter, whereas Cm-H_2O distances are longer compared to the AIMD results of Heathman et al. [17], possibly originating from the slightly different ionic radii of Eu(III) and Cm(III). To form the 1:2 complex, the nitrogen atoms entirely detach from the Cm bond with distances larger than 3.5 Å. Through charge compensation in the hydroxide complexes, the nitrogen bonding is weaker than in the corresponding only water-containing complexes (see Table 3). Otherwise, the water- and hydroxide-containing complexes remain structurally similar with or without Na^+ ions.

For all Cm(III)-EDTA species the 8-fold coordinated ion turned out to be the most stable (see Table 1). In particular the $[Cm(H_2O)_3(EDTA)]^-$ was not a structural minimum, in agreement with the average number of 2.1 H_2O molecules obtained from the Kimura equation on the fluorescence lifetime of the species. Accordingly, structures with two water molecules (or one water molecule and one hydroxide ion) were considered in Equations (3)–(6). To account for the prevailing pH in the system, reaction energies corresponding to the given equations were computed starting from $Cm(OH)^{2+}$ and H_2EDTA^{2-} as main initial species in the investigated boundary conditions. Resulting energies and stability constants are shown in Tables 1 and 2. Structural parameters are summarised in the supporting information (tables SI.1, SI.2). Calculated log K values are commonly higher than experimentally determined ones, just as in the present case, where for the formation constant of the species $Cm(EDTA)^-$, $\log^0 \beta$ values of 17.1 [31] and 20.43 [9] can be found in the literature (compared to the analogous, transformed value of $\log \beta^0 = 51.94$ calculated from Table 1, corresponding to the chemical reaction $Cm^{3+} + EDTA^{4-} \rightleftharpoons Cm(EDTA)^-$). It is, however, important to note that calculated stability constants offer a basis for comparing relative stabilities and depicting trends along a series of similar species. Computed values of stability constants: $\log K_{H2O} = 41.1$ versus $\log K_{OH} = 42.3$ for the corresponding reactions favour the formation of the hydroxo-complex over the $Cm(EDTA)^-(aq)$, especially under alkaline conditions. For the 1:2 Cm:EDTA stoichiometric ratios, the fully deprotonated species $[Cm(EDTA)_2]^{5-}$ was determined to be a global minimum with a negative associated Gibbs formation energy. Hence, at sufficiently high EDTA concentrations, the latter species could become predominant, as it was also reported to form for Am(III) by Delle Site et al. [12] above 5 mM EDTA total concentration. The $Cm(EDTA)_3^{6-}$ was also shown to be an energetic minimum according to our calculations (see SI Figure 4 for structure), but its significantly lower

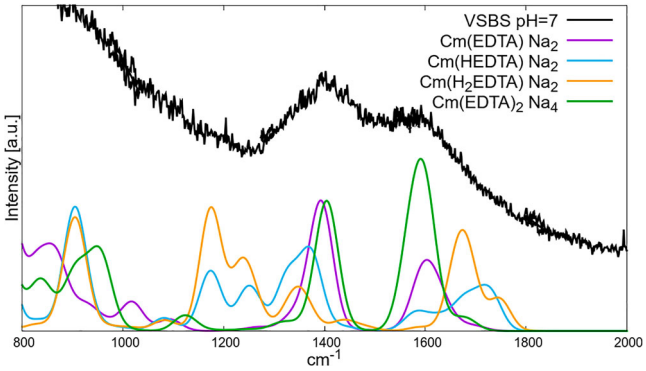


Figure 4. Vibronic side-band spectrum (black, pH = 7) and computed spectra for various Cm(EDTA) complexes.

Table 1. Calculated Gibbs free energies in kJ/mol for the formation of the $[Cm(H_2O)_n(H_mEDTA)]^{m-1}$ and $[Cm(H_mEDTA)_2]^{2m-5}$ complexes Equations (3) & (4) and corresponding stability constants at $T = 298\,K$ assuming H_2EDTA in solution.

	ΔH	$-T\Delta S$	ΔG	log K
1:1 Equation (3)				
$m = 0, n = 2$	−25.9	−53.7	−234.8	41.1
$m = 1, n = 2$	−9.3	−25.6	−217.9	38.2
$m = 2, n = 2$	8.2	9.9	−133.3	23.4
$m = 2, n = 3$	8.6	12.6	−131.5	23.0
$m = 4, n = 2$	39.2	77.4	80.3	−14.1
$m = 4, n = 3$	39.5	79.1	114.8	−20.1
1:2 Equation (4)				
$m = 0$	−41.9	−36.4	−6.4	1.1
$m = 2$	−2.9	45.7	26.2	−4.6
$m = 4$	49.4	125.5	118.8	−20.8

Table 2. Calculated Gibbs free energies in kJ/mol for the formation of the $[Cm(OH)(H_2O)(H_mEDTA)]^{(m-2)}$ complexes Equation (5) and corresponding stability constants at $T = 298K$ assuming H_2EDTA in solution.

	ΔH	$-T\Delta S$	ΔG	log K
1:1				
$m = 0$	−47.2	−97.2	−241.5	42.3
$m = 2$	−10.3	−26.6	−119.2	20.9
$m = 4$	24.6	43.8	35.8	−6.3

associated stability constant suggests a rather minor contribution to the speciation distribution of Cm(III) in the presence of EDTA.

The Na^+ ions stablise hydroxo groups in the ternary $Cm(OH)_n(EDTA)^{-1-n}$ structures. Among the different possible configurations we found three stable structures: $[Cm(OH)(H_2O)(EDTA)]^{2-}\cdot[(Na(H_2O)_4)_2]^{2+}$, $[Cm(OH)_2(EDTA)]^{3-}\cdot[(Na(H_2O)_4)_4]^{4+}$ and $[Cm(OH)(H_2O)(EDTA)]^{2-}\cdot[(Na(H_2O)_4)_3]^{3+}$. The latter structure is shown in Figure 3, the others in the supporting information (Figures SI.2 and SI.3). No energetic minima were found for $Cm(OH)_n(EDTA)^{-1-n}$ with $n \geq 3$ could be found.

Table 3. Average Cm bond distances in Å of the Na^+-saturated $Cm(OH)(H_2O)(EDTA)$ complexes.

	d_O	d_N	d_{H_2O}	d_{OH}
$[Cm(H_2O)_2(EDTA)]^-\cdot[(Na(H_2O)_4)_2]^{2+}$	2.38	2.70	2.53	
$[Cm(H_2O)_2(HEDTA)]\cdot[Na(H_2O)_4]^+$	2.39	2.71	2.55	
$[Cm(H_2O)_2(H_2EDTA)]^+\cdot[Na(H_2O)_4]^+$	2.40	2.73	2.57	
$[Cm(EDTA)_2]^{5-}\cdot[(Na(H_2O)_4)_4]^{4+}$	2.41	3.51		
$[Cm(OH)(H_2O)(EDTA)]^{2-}\cdot[(Na(H_2O)_4)_2]^{2+}$	2.40	2.85	2.57	2.29
$[Cm(OH)(H_2O)(EDTA)]^{2-}\cdot[(Na(H_2O)_4)_3]^{3+}$	2.40	2.81	2.67	2.32
$[Cm(OH)_2(EDTA)]^{3-}\cdot[(Na(H_2O)_4)_4]^{4+}$	2.41	2.80		2.42

3.4. Computed vibrational spectra

Figures 4 and 5 depict the computed spectra for some aqueous 1:1 and 1:2 EDTA complexes against the experimental spectra at pH = 7 and 12, respectively. CN vibrations are determined at 920 cm^{-1}. CO vibrations split into two separate features around 1400 and 1610 cm^{-1}. The splitting increases with increasing protonation of the coordinated ligand. Water bending modes are determined to be located around 1650 cm^{-1}. In comparison with the experimentally gained spectra at pH = 7, only the 1:1 and 1:2 complexes with a fully deprotonated EDTA ligand were found to be in good agreement. Following the relatively large difference in the calculated stability constants of the two species and the applied $[EDTA]_{tot} = 10^{-3}M$, spectral features at pH = 7 most likely correspond to the presence of the $Cm(EDTA)^-$ species in solution. Identifiable features in the spectra at pH = 12 are in accordance with the computed vibronic side bands for the Na^+-stabilised hydrolysed species. The addition of Na^+ ions to the moieties was found to be crucial for the description of the VSB positions as in the absence of counterions, shifts of up to 150 cm^{-1} were observed for the vibronic couplings (results not shown here). As the sodium total concentration suffers a large variation along the series and spectral characteristics cannot be resolved, the exact stoichiometry of the prevailing species remains unknown. Accounting for the observed shifts in VBS positions from pH = 7 to 12 and the intensity increase of the collected spectra, however, the competition between different counterion-stabilised, hydrolysed species is underlined.

4. Conclusion

The present work represents a combined, experimental and theoretical investigation on the complexation of Cm(III) with EDTA in alkaline, aqueous solutions using time-resolved laser fluorescence spectroscopy, vibronic side-band spectroscopy and quantum chemistry. The

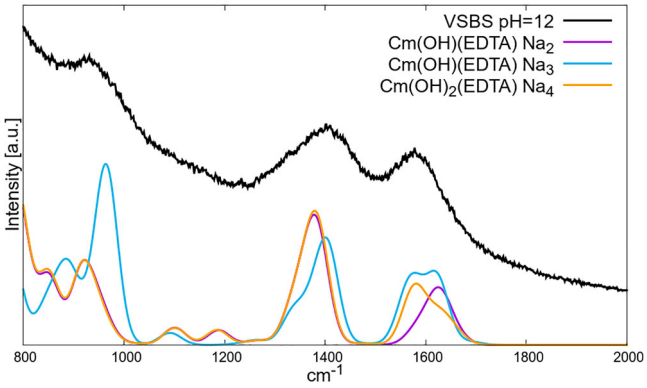


Figure 5. Vibronic side-band spectrum (black, pH = 12) and computed spectra for various hydrolysed Cm(EDTA) complexes.

pH-dependent, normalised TRLFS spectral series displayed one isosbestic point with increasing pH, indicating the predominance of two main species located at 603.9 and 606.9 nm. Trends in computed log K values for various $Cm(OH)_n(H_mEDTA)^{m-n-1}$ species revealed the increased stability of the deprotonated species and the prominent stability of $Cm(OH)(EDTA)^{2-}$ species expectedly related to the emerging TRLFS signal at 606.9 nm. Upon further increase in alkalinity, the presence of a third, potentially hydrolysed Cm-EDTA species was also visible at 613.9 nm, which was confirmed by quantum chemical calculations to be most likely the $Cm(OH)_2(EDTA)^{3-}$ species. Comparison of recorded and computed vibronic side-band spectra proved that EDTA must predominantly exist in fully deprotonated state as coordinated to the Cm(III) centre within the complexes. Derived stoichiometries were further underlined by the excellent agreement between the experimental and theoretical spectral features of the vibrational side bands. The present study provides unequivocal proof for the formation of hydrolysed, Cm(III)-EDTA species dominating the speciation of Cm(III) in the millimolar level of EDTA concentrations under alkaline conditions. The existence of a complex with 1:2 Cm to EDTA stoichiometry cannot be excluded, although the formation of this complex expectedly requires a large excess of the ligand in solution. Based on their similarities in terms of ionic radii, analogous stoichiometries and relative stabilities can be predicted for the complexes of EDTA with other trivalent actinides, e.g. Am^{3+} or Pu^{3+} ($r_{Cm3+} = 1.09$ Å, $r_{Am3+} = 1.10$ Å, $r_{Pu3+} = 1.12$ Å, all of them with CN = 8) [32]. The results obtained in this work provide key insights for the accurate description of the An(III)-EDTA systems under boundary conditions of relevance in nuclear waste and environmental applications.

Acknowledgments

This research was supported, in part, by an appointment to the DOE Scholars Program (N.A. DiBlasi), sponsored by the U.S. Department of Energy, administered by the Oak Ridge Institute for Science and Technology, and funded by the WIPP Project (DOE-CBFO, contact Donald T. Reed).

Disclosure statement

No potential conflict of interest was reported by the author(s).

Funding

This research was supported, in part, by an appointment to the DOE Scholars Program (N.A. DiBlasi), sponsored by the U.S. Department of Energy, administered by the Oak Ridge Institute for Science and Technology, and funded by the WIPP Project (DOE-CBFO, contact Donald T. Reed).

ORCID

M. Trumm http://orcid.org/0000-0002-6193-6780

References

[1] J. Fuger, J. Inorg. Nucl. Chem. **5**, 332–338 (1958). doi:10.1016/0022-1902(58)80011-1
[2] I. Lebedev, A. Maksimova, A. Stepanov and A. Shalinets, Sov. Radiochem. **9**, 664–666 (1967).
[3] A. Stepanov, Russ. J. Inorg. Chem. **16**, 1583–1586 (1971).
[4] A. Shalinets, Sov. Radiochem. **14**, 285–289 (1972).
[5] G. Choppin, Q. Liu and J. Sullivan, Inorg. Chem. **24**, 3968–3969 (1985). doi:10.1021/ic00217a054
[6] K. Cernochovaa, J. Mathur and G. Choppin, Radiochim. Acta. **93**, 733–739 (2005). doi:10.1524/ract.2005.93.12.733
[7] P. Thakur, J. Conca, L.V. de Burgt and G. Choppin, J. Coord. Chem. **62**, 3719–3737 (2009). doi:10.1080/00958970903183909
[8] T. Griffiths, L. Martin, P. Zalupski, J. Rawcliffe, M. Sarsfield, N. Evans and C. Sharrad, Inorg. Chem.**52**, 3728–3737 (2013). doi:10.1021/ic302260a
[9] P. Thakur, Y. Xiong, M. Borkowski and G. Choppin, Geochim. Cosmochim. Acta. **133**, 299–312 (2014). doi:10.1016/j.gca.2013.09.040
[10] A. Moskvin, G. Khalturin and A. Gel'man, Sov. Radiochem. **1**, 69–76 (1960).
[11] I. Stary, Sov. Radiochem. **8**, 467–470 (1966).
[12] A.D. Site and R. Baybarz, J. Inorg. Nucl. Chem. **31**, 2201–2233 (1969). doi:10.1016/0022-1902(69)90039-6
[13] A. Elesin and A. Zaitsev, Sov. Radiochem. **13**, 798–801 (1971).
[14] W. D'Olieslager and G. Choppin, Inorg. Nucl. Chem. **33**, 127–135 (1971). doi:10.1016/0022-1902(71)80016-7
[15] G. Korpusov, E. Patrusheva, M. Dolidze and A. Trubnikova, Sov. Radiochem. **17**, 496–501 (1975).
[16] J.-F. Chen, G.R. Choppin, and R.C. Moore, in: *Actinide speciation in high ionic strength media*, (1999).
[17] C. Heathman, T. Grimes, S. Jansone-Popva, S. Roy, V. Bryantsev and P. Zalupski, Chem. Eur. J. **25**, 2545–2555 (2019). doi:10.1002/chem.v25.10
[18] C. Lee, W. Yang and R. Parr, Phys. Rev. B: Condens. Matter. **37**, 785–789 (1988). doi:10.1103/PhysRevB.37.785

[19] A. Becke, J. Chem. Phys. **98**, 5648–5652 (1993). doi:10.1063/1.464913
[20] W. Küchle, M. Dolg, H. Stoll and H. Preuss, J. Chem. Phys. **100**, 7535–7542. (1994). doi:10.1063/1.466847
[21] *Turbomole v7.1, a development of University of Karlsruhe and forschungszentrum karlsruhe gmbh, 1989–2007, turbomole gmbh*, since 2007. < www.turbomole.com > .
[22] A. Klamt and G. Schüürmann, J. Chem. Soc. Perkin Trans. **2**, 799 (1993. doi:10.1039/P29930000799
[23] N. Heinz, J. Zhang and M. Dolg, J. Chem. Theory Comput. **10**, 5593–5598 (2014). doi:10.1021/ct5007339
[24] V. Bryantsev, M. Diallo and W. Goddard, J. Phys. Chem. **112**, 9709–9719 (2008). doi:10.1021/jp802665d
[25] T. Fanghänel, J. Kim, P. Paviet, R. Klenze and W. Hauser, Radiochim. Acta. **66–67**, 81–88 (1994). doi:10.1524/ract.1994.6667.special-issue.81
[26] T. Kimura, G. Choppin and Y. Kato, Radiochim. Acta. **72**, 61–64 (1996). doi:10.1524/ract.1996.72.2.61
[27] D. Rai, D. Moore, K. Rosso, A. Felmy and H. Bolton, J Solution Chem. **37**, 957–986 (2008). doi:10.1007/s10953-008-9282-2
[28] Y. Xia, A. Felmy, L. Rao, Z. Wang and N. Hess, Radiochim. Acta. **91**, 751–760 (2003). doi:10.1524/ract.91.12.751.23416
[29] E. Giffaut, M. Grivé, P. Blanc, P. Vieillard, E. Colàs, H. Gailhanou, S. Gaboreau, N. Marty, B. Madé and L. Duro, Appl. Geochem. **49**, 225–236 (2014). doi:10.1016/j.apgeochem.2014.05.007
[30] *Infrared spectra' by NIST mass spectrometry data center*, William E. Wallace, Director, (2004).
[31] A.E. Martell and R.M. Smith, *Nist critically selected stability constants of metal complexes database*, version 8.0 (2004).
[32] V. Neck and J. Kim, Radiochim. Acta. **89**, 1–16 (2001). doi:10.1524/ract.2001.89.1.001